

Long non-coding RNA expression profiling in the lungs of pulmonary arterial hypertension rats with acute inflammation

Yue Yang^{1*}, Yanan Cao^{1*}, Gang Qin¹, Lu Wang¹, Qian Li¹, Sisi Dai¹, Lizhe Guo¹, Qulian Guo¹, Yong Gang Peng², Bin Duan¹ and E. Wang¹ 

¹Department of Anesthesiology, Xiangya Hospital, Central South University, Changsha, People's Republic of China; ²Department of Anesthesiology, University of Florida College of Medicine, Gainesville, FL, USA

Abstract

Background: We performed RNA-sequencing to investigate the changes and expression profiles in long non-coding RNAs (lncRNAs) and their potential functional roles in the lungs of pulmonary arterial hypertension rats responding to acute inflammation.

Methods: To establish a pulmonary arterial hypertension rat model, monocrotaline was injected intraperitoneally and lipopolysaccharide was given to induce acute inflammation. Selected lncRNAs were validated by quantitative real-time polymerase chain reaction (qRT-PCR). Bioinformatics analyses were carried out to predict the potential biological roles of key lncRNAs.

Results: Twenty-eight lncRNAs and seven mRNAs with elevated expression and 202 lncRNAs and 36 mRNAs with decreased expression were found in the lung tissues of lipopolysaccharide-treated pulmonary arterial hypertension rats compared with control group. The qRT-PCR validation results were consistent with the bioinformatics analysis. Gene ontology analyses showed that the mRNAs and lncRNAs were differentially expressed in different pathways regarding biological process, cellular components, and molecular function. The functions of differentially expressed messenger RNAs (DEmRNAs) and DELncRNAs were indicated by Kyoto Encyclopedia of Genes and Genomes enrichment.

Conclusion: The DEmRNAs co-expressed with DELncRNAs were obviously enriched in inflammation. DELncRNAs and DEmRNAs in the lungs of pulmonary arterial hypertension rats changed with acute inflammation may provide new insights into the pathogenesis of pulmonary arterial hypertension.

Keywords

pulmonary arterial hypertension, long non-coding RNAs, messenger RNA, lung, inflammation

Date received: 4 May 2019; accepted: 7 September 2019

Pulmonary Circulation 2019; 9(4) 1–10

DOI: 10.1177/2045894019879393

Background

Pulmonary arterial hypertension (PAH) is a progressive pulmonary vasculature pathological alteration that is characterized by an extreme increase in pulmonary vascular resistance, pulmonary arterial pressure, and possible right ventricular hypertrophy.¹ Research has shown that histological lung tissue from a PAH model displayed critical vascular remodeling.² Inflammation plays a critical role in the dysfunction of pulmonary arterial endothelial cells, but its specific mechanism remains inconclusive.³ It has been observed that when severe PAH becomes acutely inflamed, cardiac function deteriorates rapidly and even leads to

death. As inflammation evidently aggravates the insult of PAH, the underlying mechanisms must be investigated.

Long non-coding RNAs (lncRNAs) are defined as non-coding transcripts with a length greater than 200 nucleotides. Substantial evidence indicates that lncRNAs interact with DNA, RNA, and proteins and play key roles

*These authors contributed equally to this study.

Corresponding author:

E. Wang, Department of Anesthesiology, Xiangya Hospital, Central South University, Changsha, Hunan 410008, China.

Email: ewang324@csu.edu.cn



Creative Commons Non Commercial CC BY-NC: This article is distributed under the terms of the Creative Commons Attribution-NonCommercial 4.0 License (<http://www.creativecommons.org/licenses/by-nc/4.0/>) which permits non-commercial use, reproduction and distribution of the work without further permission provided the original work is attributed as specified on the SAGE and Open Access pages (<https://us.sagepub.com/en-us/nam/open-access-at-sage>).

© The Author(s) 2019.
Article reuse guidelines:
sagepub.com/journals-permissions
journals.sagepub.com/home/pul



in many important biological processes, such as transcription regulation, post-transcription regulation, and epigenetic regulation.^{4,5} Studies show the rs619586A > G single nucleotide polymorphism is correlated with risk of PAH. People with G variant genotypes have a lower risk of PAH compared to the rs619586AA genotype.⁶ Differential expressions of lncRNAs were observed in chronic thromboembolic pulmonary hypertension tissues and in the hypoxic PAH rat model.^{7,8} What is less well known, however, is how lncRNAs change and what their potential function is in lung tissues of lipopolysaccharide (LPS)-treated PAH rats.

In our study, lncRNAs and mRNA expression profiling of PAH rats in circumstances of acute inflammation were obtained through high-throughput sequencing. DElncRNAs and DE mRNAs in lungs were identified, and we also constructed an lncRNA/mRNA co-expression network. This is the first comprehensive lncRNA profile in lungs of LPS-treated PAH rats.

Methods

Animal experiments

All procedures involving animals were authorized by the Ethics Committee for Animal Research of Xiangya Hospital of Central South University (approval no. 201303311). Twenty male Sprague-Dawley rats weighted 250–300 g were purchased from the Laboratory Animal Center of Central South University (Changsha, China). To induce PAH, 1% monocrotaline (60 mg/kg, Sigma-Aldrich, St. Louis, MO, USA) was intraperitoneally injected to all rats. Rats had free access to food and water and were given a 12-h light/dark cycle in a temperature-controlled room. After 28 days, pulmonary arterial pressure was measured by echocardiography using the method of tracing the tricuspid regurgitation spectrum. If the pulmonary arterial pressure was ≥ 60 mmHg, the rats were included in the next experiment. Then, the rats were divided into two groups randomly: PAH group and PAH+LPS group. LPS (1 mg/kg) (Serotype O55:B5, Sigma-Aldrich) was intraperitoneally injected to rats in the PAH+LPS group. Two hours later, the rats were sacrificed via exsanguination under ketamine anesthesia, and lung tissues were harvested for RNA isolation.

High-throughput sequencing

Total RNA of the lung tissues from three PAH rats and three PAH rats treated with LPS were extracted using TRIZOL reagent (Invitrogen, Grand Island, NY, USA). The high-throughput sequencing work was carried out by Genergy Biotechnology (Shanghai, China). First, the RNA quality and quantity were measured by Nanodrop (Thermo Fisher Scientific, Waltham, MA, USA). Then, 1 μ g of total RNA was amplified and transcribed into ds cDNA and constructed RNA library by Quant-iT™

PicoGreen® dsDNA Assay Kit (Life Technologies, Carlsbad, CA, USA) and Qubit (Invitrogen). After clustering generation with cBot (Illumina, San Diego, California, USA), the arrays were scanned by the HiSeq2500 SBS (Illumina), and the raw data were subsequently processed. DElncRNAs and DE mRNAs were filtered by fold-change.

Quantitative real-time PCR

The results of high-throughput sequencing analysis were verified by quantitative real-time polymerase chain reaction (qRT-PCR). Total RNA was extracted by using TRIZOL reagent (Invitrogen) and then cDNA was synthesized by a PrimeScript™ RT reagent Kit (Takara Bio Inc., Otsu, Japan). The online primer design website, primer3 (<http://primer3.ut.ee/>) was used to design the specific promoter primers. The following primers were used:

TCONS_00321934, forward, CACGGCAAGACCAAGA CAGA, reverse, TTCTCCCACGGCATTCTCTCG; TCONS_00196921, forward, AAGGAAGCCCATAACGGTC AG, reverse, TCTCTGTCTCTGTGTCTCTGGT; TCONS_00107023, forward, CAGTGGCGGTGGTGATAACA, reverse, GGTTGGAGGCTGGTGAGTTC; TCONS_00243128, forward, GGCATCTGTCTGTAGGTGGTC, reverse, TTTGCTCTCCTGGGCTTGTTT; Cxcl-6, forward, CGGTCTGCTCGTCATTAC, reverse, CGTAGCTCCGTTGCAACCAT; Il-6, forward, CCAGTTGCCTTCTTGGGACTG, reverse, TTGTGGGTGGTATCCTCTGTGA; Lbh, forward, GAACCCACAGAAGGGGAGGT, reverse, TGTCTGCTCATCCTCCTGG; Rtn2, forward, CCGCTTTGATCTCAGCATTGA, reverse, GGATCCTCCTCCCGACCAA; GAPDH, forward, TGATTCTACCCACGGCAAGTT, reverse, TGATGGGTTTCCCATTGATGA.

qRT-PCR was performed to detect lncRNA and mRNA expression in lungs with ABI Prism 7900 Sequence Detection System (Applied Biosystems, Foster City, CA). Conditions for amplification were at 94°C for 1 min and 40 cycles of 95°C for 10 s, 60°C for 30 s and 72°C for 30 s. Each reaction was done in triplicate. Transcript levels of each lncRNA normalized to GAPDH were calculated using the $2^{-\Delta\Delta CT}$ method.

Functional group analysis

The functions of DE genes were detected by Gene ontology (GO) analysis. GO analysis can classify genes into hierarchical categories along biological processes, molecular functions, and cellular component and reveal gene regulatory networks. Kyoto Encyclopedia of Genes and Genomes database (KEGG) was used to analyze pathway. Two-sided Fisher's exact test was used to analyze data, and false discovery rate was calculated and *P* value was corrected. *P* < 0.05 was considered statistically significant.

Co-expression network

To confirm lncRNAs involved in the pathogenesis of acute right ventricular failure in LPS-treated PAH rats, we selected DEmRNAs detected in this study to build a co-expression network. A Pearson correlation coefficient (PCC) was figured between the top 10 upregulated/down-regulated DElncRNAs and detected mRNAs. A $PCC \geq 0.99$ was considered as a significant correlation pair.

Statistical analysis

All data were presented as mean \pm standard deviation. Differences between groups were determined by Student's t-test ($P < 0.05$ was considered statistically significant). All results were processed using GraphPad Prism 6 Software (GraphPad, La Jolla, CA, USA).

Results

RNA sequencing of lung tissues from LPS-treated PAH rats

Lung tissues of PAH rats with or without LPS treatment were applied for RNA sequencing. After trimming raw reads, 1.64×10^8 , 0.64×10^8 , and 1.13×10^8 clean reads were selected from samples of LPS-treated PAH rats, respectively, and 1.16×10^8 , 1.11×10^8 , and 1.10×10^8 clean reads were selected from control tissue from three

paired PAH rats (Supplemental Table 1). Clean reads of each sample were aligned to the human reference genome. The mapped ratio of each sample was greater than 90% (Supplemental Table 2).

DElncRNAs and DEmRNAs in LPS-treated PAH rats

A total 94 up- and 258 down-regulated DElncRNAs were identified in LPS-treated PAH rats. And 445 mRNAs were upregulated and 877 mRNAs were down-regulated when compared with non-inflamed control PAH rats. Respectively, 43 DElncRNAs (36 up-regulation and 7 down-regulation) and 230 DEmRNAs (202 up-regulation and 28 down-regulation) were detected in the lung tissues of LPS-treated PAH rats compared to non-inflamed control rats in accordance with the threshold of $P < 0.05$ and $|\log_2 \text{Fold change}| \geq 2$. According to the location and transcriptional orientation, a total of 43 DElncRNAs were divided into five categories: intergenic (27, 62.8%), antisense (8, 18.6%), intronic (3, 7.0%), bidirectional (1, 2.3%), and unclassified (4, 9.3%) (Fig. 1a).

The top 10 DElncRNAs and DEmRNAs (upregulation and down-regulation) are presented in Tables 1 and 2, respectively. Hierarchical clustering of the expression of top 10 DElncRNAs and DEmRNAs (upregulation and down-regulation) show that there was obvious discrimination between LPS-treated PAH and non-inflamed control rats (Fig. 1b and c). The expression of TCONS_00107024

Table 1. Deregulated lncRNAs identified by the microarray in PAH rat with a status of acute inflammation.

lncRNAs	Chromosome	Position	FC (log2)	P
XLOC_074419	14	18745752–18784361	3.51	0.00005
XLOC_139911	2	56162113–56163131	3.43	0.0352
XLOC_266898	8	6013206–6076598	3.26	0.00005
XLOC_004526	1	69485517–69494373	2.87	0.00175
XLOC_074419	14	18745752–18784361	2.85	0.00005
XLOC_034025	10	106973874–106976040	2.84	0.00005
XLOC_099555	16	31187149–31194242	2.83	0.00005
XLOC_141804	2	248219427–248263168	2.8	0.00005
XLOC_268301	8	132665926–132753292	2.79	0.00005
XLOC_108967	17	8811977–8840976	2.66	0.0021
XLOC_140661	2	134217099–134275852	–3.17	0.00005
XLOC_058333	12	24974340–25021863	–2.91	0.03365
XLOC_005738	1	156444464–156457900	–2.46	0.0059
XLOC_138438	2	190946625–191044228	–2.19	0.0003
XLOC_233416	6	24160225–24184120	–2.14	0.00005
XLOC_282901	9	70010577–70037631	–2.08	0.0175
XLOC_174435	3	52875784–52877295	–2.01	0.02115
XLOC_139873	2	53580678–53602678	–1.99	0.00005
ENSRNOG00000055537	6	142404864–142405483	–1.99	0.0001
ENSRNOG00000058261	3	18653319–18654383	–1.97	0.00005

and TCONS_00198427 varied most significantly in DElncRNAs. The expression of Cxcl10 and Lbh varied most significantly in DEmRNAs.

qRT-PCR validation of DElncRNAs

To validate the reliability of RNA-seq results, DElncRNAs and DEmRNAs were selected for further qRT-PCR verification. Four DElncRNAs and four mRNAs were chosen for verification. TCONS_00196921 and TCONS_00107023 were upregulated in LPS-treated PAH rats compared with the control rats ($P < 0.01$). TCONS_00321934 ($P < 0.05$) and TCONS_00243128 ($P < 0.01$) were significantly down-regulated in LPS-treated PAH rats compared with control group. Cxcl6 ($P < 0.01$) and Il-6 ($P < 0.01$) were upregulated, whereas Lbh ($P < 0.001$) and Rtn2 ($P < 0.01$) were down-regulated ($P < 0.05$) significantly in the lung tissues of LPS-treated PAH rats (Fig. 2).

GO and KEGG pathway enrichment

We found that 230 mRNAs were differentially expressed. The upregulated mRNAs were enriched in TNF signaling pathway (KEGG: 04668), cytokine-cytokine receptor interaction (KEGG: 04060), NF-KB signaling pathway (KEGG: 04064), chemokine signaling pathway (KEGG: 04062), malaria (KEGG: 05144). The down-regulated mRNAs were enriched in Hippo signaling pathway

(KEGG: 04390), systemic lupus erythematosus (KEGG: 05322), transcriptional misregulation in cancer (KEGG: 05202), basal cell carcinoma (KEGG: 05217), and cGMP-PKG signaling pathway (KEGG: 04022) (Fig. 3). The important KEGG pathways were found with a P value < 0.05 , and they were ranked according to their enrichment scores ($-\log_{10}(P\text{-value})$). Furthermore, those upregulated mRNAs were significantly enriched in defense response, response to cytokine, immune system process, extracellular space, extracellular region part, cell surface, chemokine receptor binding, chemokine activity, cytokine activity of GO molecular function, cellular component, and biological process, and the downregulated mRNAs were enriched in cardiovascular system development, circulatory system development, multicellular organismal development, protein-DNA complex, actomyosin, nucleosome, protein heterodimerization activity, protein binding, and phosphatidylinositol 3-kinase activity (Fig. 4).

Co-expression network among lncRNAs and coding genes

We calculated the PCC on the basis of the expression of DElncRNAs and DEmRNAs to investigate the potential functions of inflammation on PAH. The top 10 upregulated/downregulated DElncRNAs and DEmRNAs were included in the co-expressed network, which contained 10 nodes and 230 edges (Fig. 5). The top five upregulated DEmRNAs were Cxcl10, Cxcl6, Csf3, Il6, and Ccl20, and

Table 2. Deregulated mRNAs identified by the microarray in PAH rat with a status of acute inflammation.

mRNA name	Symbol	Regulation direction	Fold change (log2)	P
ENSRNOT0000003075	Cxcl10	Up	6.41	0.00005
ENSRNOT0000003823	Cxcl6	Up	5.90	0.00005
ENSRNOT00000011509	Csf3	Up	5.89	0.0151
ENSRNOT00000013732	Il6	Up	5.50	0.00005
ENSRNOT00000021730	Ccl20	Up	5.42	0.00005
ENSRNOT00000022827	Pla2g2a	Up	5.40	0.00005
ENSRNOT00000016541	Ptx3	Up	5.27	0.00005
ENSRNOT00000003778	Cxcl1	Up	5.20	0.00005
ENSRNOT00000003759	Selp	Up	5.16	0.00005
ENSRNOT00000003745	Cxcl2	Up	5.06	0.00005
ENSRNOT00000071312	AABR07027447.1	Down	-3.56	0.0002
ENSRNOT00000063989	B230307C23Rik	Down	-3.07	0.0057
ENSRNOT00000091904	Lbh	Down	-3.02	0.00005
ENSRNOT00000061284	Lbh	Down	-2.82	0.0005
ENSRNOT00000014346	Wisp2	Down	-2.72	0.00005
ENSRNOT00000016984	Vamp5	Down	-2.70	0.035
ENSRNOT00000068778	Rtn2	Down	-2.67	0.00005
ENSRNOT00000071806	Cldn5	Down	-2.64	0.00005
ENSRNOT00000006203	Fibin	Down	-2.60	0.00005
ENSRNOT00000020528	Ctgf	Down	-2.45	0.00005

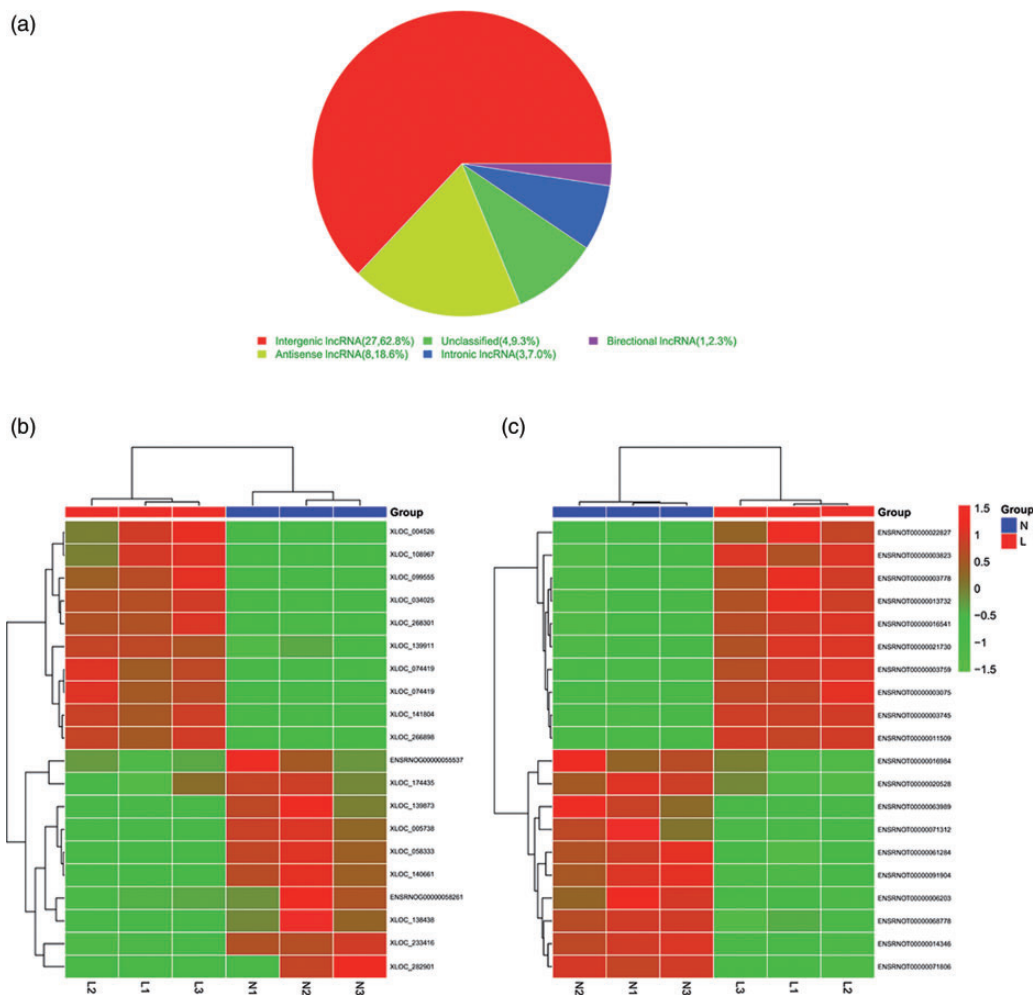


Fig. 1. Distribution of deregulated long non-coding RNAs (lncRNAs) and heatmaps in pulmonary arterial hypertension (PAH) rats with acute inflammation and in the control group. (a) lncRNAs were divided into five categories: intergenic, antisense, intronic, bidirectional, and unclassified according to their relationships with protein-coding genes. (b) Heatmap showing differentially expressed lncRNAs (DElncRNAs) from lung tissues of PAH rats with acute inflammation compared with lung tissues of PAH control rats. (c) Heatmap showing differentially expressed mRNA (DEmRNA) from lung tissues of PAH rats with acute inflammation compared with lung tissues of PAH control rats. Row and column represent DElncRNAs/DEmRNAs and tissue samples. The color scale indicates \log_{10} fragments per kilobase million of the expression levels of DElncRNAs/DEmRNAs. Red and green indicate up- and down-regulation. N represents PAH rats without inflammation and L represents PAH rats with acute inflammation.

these mRNAs were mostly associated with inflammation. The down-regulated expressed DEmRNAs were *Cldn5*, *Rtkn2*, *Vamp5*, *Wisp2*, and *Lbh*, and so on. These genes are associated with cell structure and function.

Discussion

Inflammation is the basis of many pathophysiological processes. Acute inflammation is the initial reaction of the body to noxious stimulation, whereas chronic inflammation is a process of long-term maladaptive response involving inflammatory activation, tissue damage, and tissue repair.⁹ Pulmonary hypertension is related with persistent inflammation and an inflammatory response that leads to pulmonary vascular remodeling and hemodynamic alteration.¹⁰ Enhancement of inflammation, apoptosis, and fibrosis

have been identified as three key biomarkers involved in an experimental model of monocrotaline-induced PAH.¹¹ However, how acute inflammation caused by infection leading to rapidly deteriorating PAH occurs remains unclear. lncRNAs are transcripts without coding protein function. Increasing evidence demonstrates that DElncRNAs are associated with multiple disease pathogenesis processes, such as tumor,¹² heart failure,¹³ and inflammation. We investigated the changes and expression profiles of lncRNAs and their potential functional in the lung tissues of LPS-treated PAH rats.

In our study, a total 94 up- and 258 down-regulated DElncRNAs were identified in LPS-treated PAH rats. In addition, 445 mRNAs were upregulated and 877 mRNAs were down-regulated in LPS-treated PAH rats. Among these, 36 upregulated lncRNAs and 7

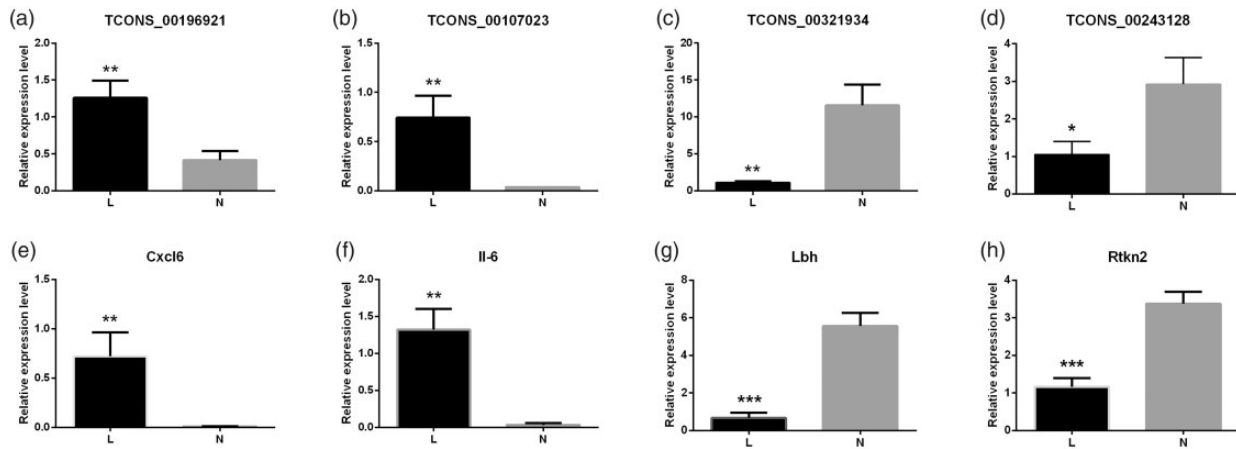


Fig. 2. Quantitative real-time PCR validation of dysregulated differentially expressed (DE) long non-coding RNAs (lncRNAs) and differentially expressed mRNAs (DEmRNAs) in pulmonary arterial hypertension (PAH) rats with acute inflammation compared with matched tissues of control PAH rats. (a) Expression level of lncRNA TCONS_00196921, (b) expression level of lncRNA TCONS_00107023, (c) Expression level of lncRNA TCONS_00321934, (d) expression level of lncRNA TCONS_00243128, (e) Expression level of Cxcl6, (f) expression level of Il-6, (g) Expression level of Lbh and (h) expression level of Rtkn2. N represents PAH rats without inflammation and L represents paired PAH rats with acute inflammation. * $P < 0.05$, ** $P < 0.01$, *** $P < 0.001$.

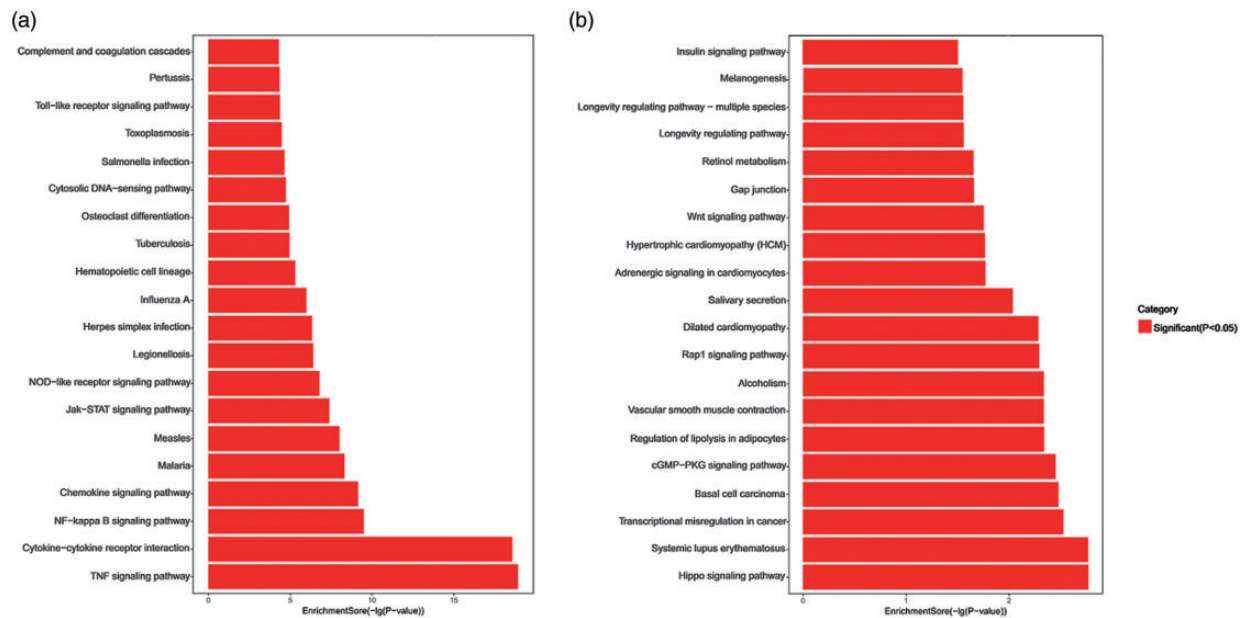


Fig. 3. Kyoto Encyclopedia of Genes and Genomes (KEGG) pathway enrichment analysis for mRNAs with the 20 highest enrichment scores. (a) KEGG pathway enrichment analysis for upregulated mRNAs. (b) KEGG pathway enrichment analysis for down-regulated mRNAs. The abscissa is $-\lg P$ -value ($-\lg P$). The bigger the $-\lg P$, the smaller the P value, indicating that the enrichment of differentially expressed genes in a given pathway was significant.

down-regulated lncRNAs, as well as 202 upregulated mRNAs and 28 down-regulated mRNAs had up to 2.0-fold change ($P < 0.05$). We selected four lncRNAs (TCONS_00196921, TCONS_00107023, TCONS_00321934, and TCONS_00243128) and four mRNAs (Cxcl6, Il-6, Lbh, and Rtkn2) for verification. The results of the qRT-PCR

analysis were in accordance with the results of high-throughput sequencing, thus indicating that the RNA-sequencing data were reliable. Thus, our study provided a profound understanding of the role of lncRNAs in LPS-treated PAH rats and throws light on the treatment of PAH patients with acute inflammation.

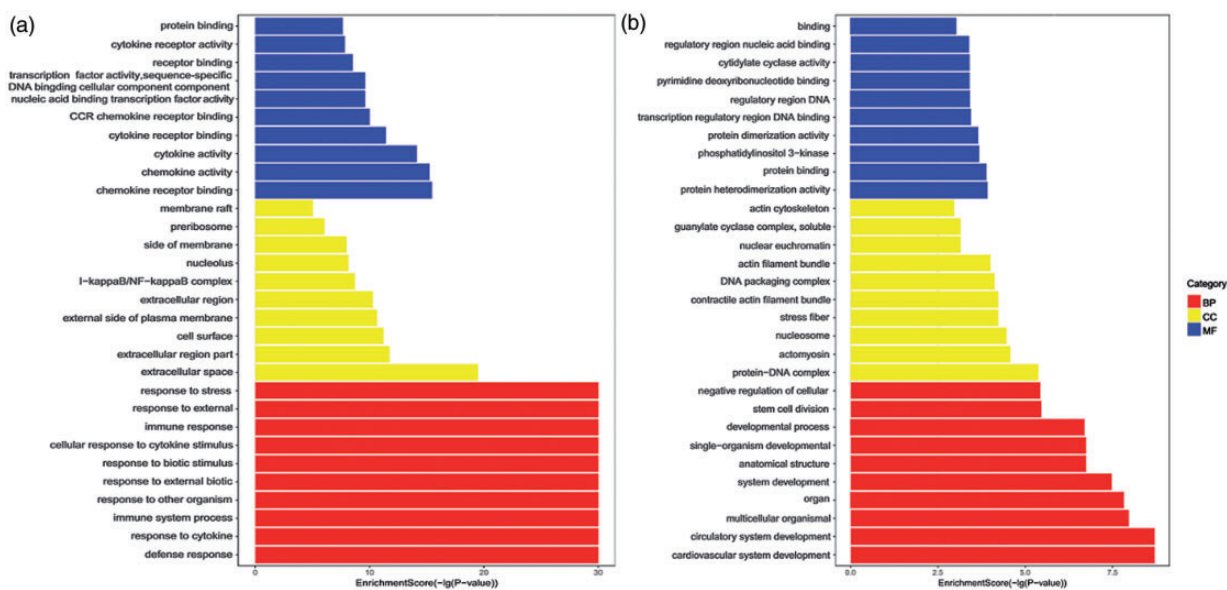


Fig. 4. Gene ontology (GO) enrichment analysis for mRNAs with the 10 highest enrichment scores. (a) GO enrichment analysis for up-regulated mRNAs, (b) GO enrichment analysis for down-regulated mRNAs. Blue bars are biological processes, green are cellular components, and red are molecular functions. The abscissa is $-\lg P$ -value ($-\lg P$). The bigger the $-\lg P$, the smaller the P value, indicating that the enrichment of differentially expressed genes in a given pathway was significant.

We performed GO term enrichment analysis to identify biological processes, cellular components, and molecular functions associated with the DElncRNAs. We found that the DElncRNAs were greatly enriched in functions related to biological process (cardiovascular system development and defense response), cell components (actomyosin and extracellular space), and molecular functions (protein heterodimerization activity and chemokine receptor binding). KEGG also highlighted the important pathways involved in the inflammation mechanism, such as vascular smooth muscle contraction, Rap1 signaling pathway,¹⁴ TNF signaling pathway, and cytokine-cytokine receptor interaction. Among these pathways, the NF- κ B signaling pathway was demonstrated to be the dominant pathway. It is well known that TNF- α increases both acute and chronic heart failure and is connected with the severity and poor outcome of heart failure.¹⁵ In the present study, many DElncRNAs in the lung tissues of LPS-treated PAH rats were found and we predicted their corresponding cis- and trans-targeting mRNAs using bioinformatic analysis. LncRNA TCONS_00198427 was predicted to act on IL-6. In PAH patients and PAH animal models, levels of the inflammatory cytokine IL-6 are elevated.^{16,17} It has been proven that IL-6 is increased in acute heart failure patients and is associated with severity and unfavorable outcomes of heart failure.^{18,19} In addition, a previous study reported that MALAT1 can raise the expression of TNF- α and IL-6 in endothelial cells.²⁰ However, the role of IL-6 and its relationship to lncRNAs has not been extensively studied. LncRNA TCONS_00107024 could interact with matrix metalloproteinase 9 (MMP-9) and tissue inhibitor of

matrix metalloproteinases 1. MMP-9 was upregulated in PAH rats with acute inflammation and it has been involved in the process of sepsis,²¹ atherosclerosis,²² and chronic obstructive pulmonary disease.²³ MMP-9 is strictly regulated by its specific inhibitor of metalloproteinase 1.²⁴ A recent study showed that the lncRNA XIST interacting with MiR-124 could affect the expression of MMP-9.²⁵ MMP-9 could cause the remodeling of the left ventricular and is involved in acute processes.^{26,27} A former clinical study also showed that brain natriuretic peptide decreased collagen synthesis and increased MMP activity.²⁸ The co-expression network among lncRNAs and coding genes showed abundant information; for instance, one study revealed that knockdown Rtn2 in vitro led to apoptosis and the inhibition of invasion.²⁹ Vamp5 was involved in docking and membrane fusion during membrane transport events.³⁰ In other words, these findings are consistent with our results and give us some clues for advanced studies to explore the connection between lncRNAs and cardiovascular disease. Furthermore, these reports suggest that these DElncRNAs may play important roles in LPS-treated PAH rats.

Our study has some limitations. We used software to predict the function of lncRNAs and the relationship between lncRNAs and mRNAs, and the construction of network and pathway analyses was based on bioinformatics analysis; thus, its validity should be tested further by carrying out designed experiments.

In conclusion, our study demonstrated that 352 lncRNAs and 1322 mRNAs were expressed differently in lung tissues of LPS-treated PAH rats. lncRNAs may

analysis. SD and LG contributed to analysis and interpretation. QG, YP, BD and EW contributed to design, supervision and revising the article. All authors read and approved the final version of the article.

Conflict of interest

The author(s) declare that there is no conflict of interest.

Ethics approval and consent to participate

All experimental procedures were approved by the Ethics Committee for Animal Research of Xiangya Hospital of Central South University (permit number: 201303311).

Funding

This work was supported by The National Natural Science Foundation of China (grant no. 81873508).

ORCID iD

E. Wang  <https://orcid.org/0000-0001-9463-9769>

Supplemental material

Supplemental material for this article is available online.

References

- Voelkel NF, Gomez-Arroyo J, Abbate A, et al. Pathobiology of pulmonary arterial hypertension and right ventricular failure. *Eur Respir J* 2012; 40: 1555–1565.
- Qin G, Luo H, Yin X, et al. Effects of sevoflurane on hemodynamics and inducible nitric oxide synthase/soluble guanylate cyclase signaling pathway in a rat model of pulmonary arterial hypertension. *Anesth Analg* 2017; 125: 184–189.
- Zhao L, Luo H, Li X, et al. Exosomes derived from human pulmonary artery endothelial cells shift the balance between proliferation and apoptosis of smooth muscle cells. *Cardiology* 2017; 137: 43–53.
- Han P, Li W, Lin CH, et al. A long noncoding RNA protects the heart from pathological hypertrophy. *Nature* 2014; 514: 102–106.
- Lee JH, Gao C, Peng G, et al. Analysis of transcriptome complexity through RNA sequencing in normal and failing murine hearts. *Circ Res* 2011; 109: 1332–1341.
- Zhuo Y, Zeng Q, Zhang P, et al. Functional polymorphism of lncRNA MALAT1 contributes to pulmonary arterial hypertension susceptibility in Chinese people. *Clin Chem Lab Med* 2017; 55: 38–46.
- Wang X, Yan C, Xu X, et al. Long noncoding RNA expression profiles of hypoxic pulmonary hypertension rat model. *Gene* 2016; 579: 23–28.
- Gu S, Li G, Zhang X, et al. Aberrant expression of long noncoding RNAs in chronic thromboembolic pulmonary hypertension. *Mol Med Rep* 2015; 11: 2631–2643.
- Pullamsetti SS, Savai R, Janssen W, et al. Inflammation, immunological reaction and role of infection in pulmonary hypertension. *Clin Microbiol Infect* 2011; 17: 7–14.
- Buendia-Roldan I, Mejia M, Navarro C, et al. Idiopathic pulmonary fibrosis: clinical behavior and aging associated comorbidities. *Respir Med* 2017; 129: 46–52.
- Yen CH, Tsai TH, Leu S, et al. Sildenafil improves long-term effect of endothelial progenitor cell-based treatment for monocrotaline-induced rat pulmonary arterial hypertension. *Cytotherapy* 2013; 15: 209–223.
- Terracciano D, Terreri S, de Nigris F, et al. The role of a new class of long noncoding RNAs transcribed from ultraconserved regions in cancer. *Biochim Biophys Acta* 2017; 1868: 449–455.
- Viereck J, Kumarswamy R, Foinquinos A, et al. Long noncoding RNA Chast promotes cardiac remodeling. *Sci Transl Med* 2016; 8: 322r–326r.
- Teo H, Ghosh S, Luesch H, et al. Telomere-independent Rap1 is an IKK adaptor and regulates NF-kappaB-dependent gene expression. *Nat Cell Biol* 2010; 12: 758–767.
- Dunlay SM, Weston SA, Redfield MM, et al. Tumor necrosis factor-alpha and mortality in heart failure: a community study. *Circulation* 2008; 118: 625–631.
- Wang L, Luo H, Qin G, et al. The impact of sevoflurane on coupling of the left ventricular-to-systemic vasculature in rats with chronic pulmonary hypertension. *J Cardiothorac Vasc Anesth* 2017; 31: 2027–2034.
- Humbert M, Monti G, Brenot F, et al. Increased interleukin-1 and interleukin-6 serum concentrations in severe primary pulmonary hypertension. *Am J Respir Crit Care Med* 1995; 151: 1628–1631.
- Boulogne M, Sadoune M, Launay JM, et al. Inflammation versus mechanical stretch biomarkers over time in acutely decompensated heart failure with reduced ejection fraction. *Int J Cardiol* 2017; 226: 53–59.
- Rauchhaus M, Doehner W, Francis DP, et al. Plasma cytokine parameters and mortality in patients with chronic heart failure. *Circulation* 2000; 102: 3060–3067.
- Puthanveetil P, Chen S, Feng B, et al. Long non-coding RNA MALAT1 regulates hyperglycaemia induced inflammatory process in the endothelial cells. *J Cell Mol Med* 2015; 19: 1418–1425.
- Wang M, Zhang Q, Zhao X, et al. Diagnostic and prognostic value of neutrophil gelatinase-associated lipocalin, matrix metalloproteinase-9, and tissue inhibitor of matrix metalloproteinases-1 for sepsis in the Emergency Department: an observational study. *Crit Care* 2014; 18: 634.
- Jacob MP. Extracellular matrix remodeling and matrix metalloproteinases in the vascular wall during aging and in pathological conditions. *Biomed Pharmacother* 2003; 57: 195–202.
- Bolton CE, Stone MD, Edwards PH, et al. Circulating matrix metalloproteinase-9 and osteoporosis in patients with chronic obstructive pulmonary disease. *Chron Respir Dis* 2009; 6: 81–87.
- Jotwani R, Eswaran SV, Moonga S, et al. MMP-9/TIMP-1 imbalance induced in human dendritic cells by *Porphyromonas gingivalis*. *FEMS Immunol Med Microbiol* 2010; 58: 314–321.

25. Xiong Y, Wang L, Li Y, et al. The long non-coding RNA XIST interacted with MiR-124 to modulate bladder cancer growth, invasion and migration by targeting androgen receptor (AR). *Cell Physiol Biochem* 2017; 43: 405–418.
26. Kelly D, Cockerill G, Ng LL, et al. Plasma matrix metalloproteinase-9 and left ventricular remodelling after acute myocardial infarction in man: a prospective cohort study. *Eur Heart J* 2007; 28: 711–718.
27. Yarbrough WM, Mukherjee R, Escobar GP, et al. Selective targeting and timing of matrix metalloproteinase inhibition in post-myocardial infarction remodeling. *Circulation* 2003; 108: 1753–1759.
28. Tsuruda T, Boerrigter G, Huntley BK, et al. Brain natriuretic peptide is produced in cardiac fibroblasts and induces matrix metalloproteinases. *Circ Res* 2002; 91: 1127–1134.
29. Liao YX, Zeng JM, Zhou JJ, et al. Silencing of RTKN2 by siRNA suppresses proliferation, and induces G1 arrest and apoptosis in human bladder cancer cells. *Mol Med Rep* 2016; 13: 4872–4878.
30. Takahashi M, Tajika Y, Khairani AF, et al. The localization of VAMP5 in skeletal and cardiac muscle. *Histochem Cell Biol* 2013; 139: 573–582.